



## Pollen-based biome reconstruction on the Qinghai-Tibetan Plateau during the past 15,000 years

Zhen Li <sup>a</sup>, Yongbo Wang <sup>a,\*</sup>, Ulrike Herzschuh <sup>b,c,d</sup>, Xianyong Cao <sup>e</sup>, Jian Ni <sup>f</sup>, Yan Zhao <sup>g</sup>

<sup>a</sup> College of Resource Environment and Tourism, Capital Normal University, Beijing 100048, China

<sup>b</sup> Alfred Wegener Institute Helmholtz Center for Polar and Marine Research, Research Unit Potsdam, Potsdam 14473, Germany

<sup>c</sup> Institute of Environmental Science and Geography, University of Potsdam, Potsdam 14476, Germany

<sup>d</sup> Institute of Biochemistry and Biology, University of Potsdam, Potsdam 14476, Germany

<sup>e</sup> Group of Alpine Paleoclimatology and Human Adaptation (ALPHA), State Key Laboratory of Tibetan Plateau Earth System, Resources and Environment (TPESRE), Institute of Tibetan Plateau Research, Chinese Academy of Sciences, Beijing 100101, China

<sup>f</sup> College of Chemistry and Life Sciences, Zhejiang Normal University, Jinhua 321004, China

<sup>g</sup> Institute of Geographic Sciences and Natural Resources Research, Beijing 100101, China

### ARTICLE INFO

Editor: Howard Falcon-Lang

**Keywords:**

Biomization

Pollen

Vegetation migration

Qinghai-Tibetan Plateau

Holocene

### ABSTRACT

Reconstruction of past vegetation change is critical for better understanding the potential impact of future global change on the fragile alpine ecosystems of the Qinghai-Tibetan Plateau (QTP). In this paper, pollen assemblages comprising 58 records from the QTP, spanning the past 15 kyrs, were collected to reconstruct biome compositions using a standard approach. Six forest biomes were identified mainly on the southeastern plateau, exhibiting a pattern of gradual expansion along the eastern margin during early to mid-Holocene times. The alpine meadow biome was separately identified based on an updated scheme, and showed notable westward expansions towards lower latitudes and higher altitudes during early Holocene times. Consistent patterns of migration could also be identified for the alpine steppe biome, which moved eastward during the late Holocene after 4 ka. As the dominant biome type, temperate steppe was distributed widely over the QTP with minor migration patterns, except for a progressive expansion to lower altitudes in the late Holocene times. The desert biome was inferred mainly as covering the northwestern plateau and the Qaidam Basin, in relatively restricted areas. The spatial distribution of the reconstructed biomes represent the large-scale vegetation gradient on the QTP. Monsoonal precipitation expressed predominant controls on the development of alpine ecosystems, while the variations in desert vegetation responded to regional moisture brought by the mid-latitude Westerlies. Temperature changes played relatively minor roles in the variations of alpine vegetation, but exerted more significant impacts on the forest biomes.

### 1. Introduction

The Qinghai-Tibetan Plateau (QTP), a unique landmass with an average altitude of over 4000 m, has been recognized as the Third Pole on Earth (Qiu, 2008) and the water tower of the Asian continent (Immerzeel et al., 2020). Additionally, as the driver and amplifier of the global climate system, the QTP plays an important role in regulating regional and even global climate changes, especially the evolution of Asian monsoon systems and the migration of mid-latitude Westerlies (An et al., 2001; Chen et al., 2020; Zhao et al., 2019). In the same period, uplift of the plateau led to the development of fragile alpine ecosystems, responding sensitively to regional climate fluctuations (Piao et al., 2019;

Verrall and Pickering, 2020; Zhao et al., 2021a). In turn, the land cover changes on the plateau could modulate the energy balance and transfer between the atmosphere and land surface (Yasunari, 2007), proposing significant feedbacks to regional climate variations (Tian et al., 2014). Therefore, investigation of past vegetation changes on the QTP would yield essential knowledge about how the alpine ecosystems respond/contribute to past climate variations (Tang et al., 2021; Zhao et al., 2011), providing necessary information for modelling/predicting climate and vegetation dynamics in the future (Claussen et al., 2001; Dallmeyer et al., 2011; Ni and Herzschuh, 2011).

The fossil pollen records contribute significantly to understanding prehistoric vegetation changes, which have been widely investigated

\* Corresponding author.

E-mail address: [yongbowang@cnu.edu.cn](mailto:yongbowang@cnu.edu.cn) (Y. Wang).

and interpreted (Edwards et al., 2017; Marquer et al., 2014). Since the 1980s, various fossil pollen sequences have been retrieved and reported in terms of vegetation/climate variations on the QTP during the Holocene epoch (see syntheses in Chen et al., 2020; Li et al., 2021a; and Tang et al., 2021). However, current studies have focused mainly on the vegetation histories at individual sites (e.g., Herzschuh et al., 2009a; Kramer et al., 2010a, 2010b; Ma et al., 2014; Zhao et al., 2007a) or restricted regional patterns, for instance, the northeastern QTP (Zhao et al., 2011) and the central QTP (Li et al., 2016). Owing to complex climatic and nonclimatic factors, the fossil pollen record at single site may not fully represent large scale vegetation variations. Consequently, the evaluation of vegetation change on a large spatial scale is of great significance for understanding vegetation responses to climate change and providing essential benchmarks for global vegetation models (Kaplan et al., 2003; Li et al., 2019a), particularly the results of quantitative vegetation reconstructions (Tang et al., 2021).

Based on the biogeographical and ecological knowledge about modern vegetation and associated pollen compositions, the biomization method was developed for quantitative vegetation reconstructions (Prentice et al., 1992, 1996), which eliminates the subjectivity in traditional pollen interpretations. Generally, biomes are defined based on characteristic plant functional types (PFTs), while the similarity score of each biome is calculated from the pollen spectrum through a standardized quantitative method (Ni et al., 2010; Prentice et al., 1998). Subsequently, the pollen spectra are transformed into biome types such that each pollen taxon will contribute quantitatively to a few biomes through the PFTs. As an effective method to quantify large-scale vegetation variations, the biomization method has been accomplished in Europe (Prentice et al., 1996) and then applied widely worldwide (e.g., Elenga et al., 2000; Izumi and Lézine, 2016; Williams et al., 2010). Accordingly, biomization-induced regional vegetation reconstructions have been accomplished in China over the past decades (Cao et al., 2019; Cheng et al., 2018; Li et al., 2019a, 2019b; Ni et al., 2010, 2014; Sun et al., 2020; Yu et al., 1998a, 1998b, 2000), although those earlier studies focused mainly on selected key time slices, i.e., the Last Glacial Maximum (18 ka) and the mid-Holocene (6 ka). In addition, current

reconstructions focused mainly on the vegetation dynamics of China or even the Asian continent, among which only limited information was acquired for the fragile alpine ecosystems on the QTP. Based on the modified global biomization scheme, vegetation on the QTP was reconstructed along with investigations of large-scale variations, for instance, the vegetation changes in China during the past 22,000 years (Ni et al., 2014), and biome changes in northern and eastern continental Asia since 40 ka BP (Tian et al., 2018).

To better understand the spatiotemporal variations in the alpine ecosystems on the QTP, fossil pollen assemblages from 58 records were collected for quantitative vegetation reconstructions based on the biomization method. Reconstructed biome sequences over the past 15 kyrs and selected key time slices were examined and evaluated, with major focus on the following questions: (1) What are the spatial and temporal patterns of vegetation changes on the QTP since the late Glacial? (2) How did the potential vegetation migrate on the QTP? and (3) What were the underlying factors that triggered the biome changes on the QTP?

## 2. Study area

The Qinghai-Tibetan Plateau (QTP, approximately 26–40°N, 73–105°E), covers an area of over 2.5 million km<sup>2</sup> with an average elevation of over 4000 m a.s.l., which is regarded as the largest landmass on Earth (Fig. 1; Qiu, 2008; Liu et al., 2022). The modern climate on the plateau is predominantly controlled by the Indian Summer Monsoon, the East Asian Summer Monsoon, and the mid-latitude Westerlies (Chen et al., 2020). The mean annual temperature on the QTP decreases from approximately 20 °C in the southeast to below –6 °C in the northwest (Sun, 1999). As the warm and humid air flows during the monsoonal season from the oceans are blocked by high mountains, an obvious gradient in mean annual precipitation appears with a decreasing trend from 2000 mm in the southeastern margin to <50 mm in the central and northwestern plateau (Sun, 1999). According to the topographic configuration and atmospheric circulation, especially the overall high elevation and associated cold/arid conditions, alpine vegetation types

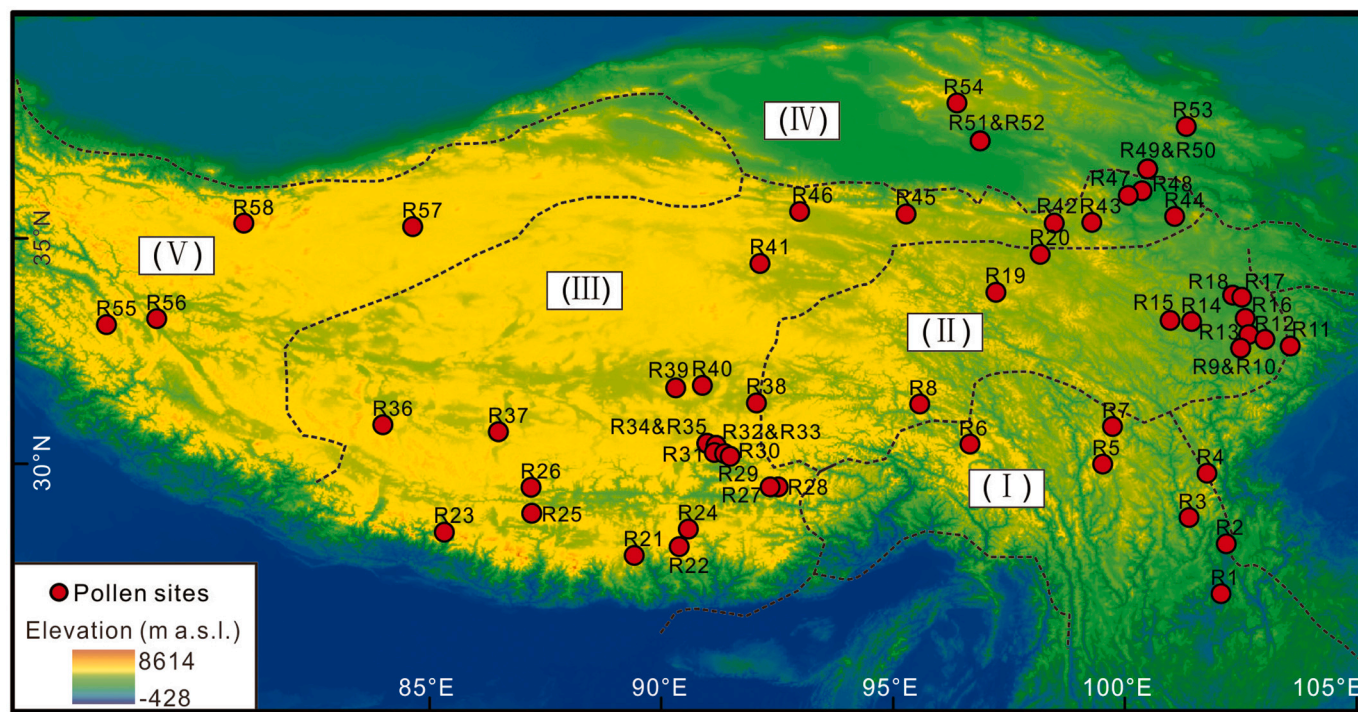


**Fig. 1.** Distribution of modern vegetation zones on the Qinghai-Tibetan Plateau and locations of fossil pollen records (see detailed information in Table 1). Vegetation zones: I, subalpine conifer forest; II, alpine meadow; III, alpine steppe; IV, temperature desert; V, alpine desert.

develop widely on the QTP (Chang, 1983; Zheng, 1996). Following the climate gradient, modern vegetation on the plateau expresses an obviously zonal pattern, from subalpine forests in the southeastern margin, to alpine meadow and scrub, alpine/temperate steppes, and alpine/temperate deserts in the northern and northwestern QTP (Fig. 1; ECVC, 1980; Hou, 2001). Generally, the dominant vegetation types on the QTP are alpine/temperate steppes, which are dominated by a mixture of plant species from Poaceae (e.g., *Stipa purpurea*) and *Artemisia* (e.g., *A. gmelinii*, *A. argyi*). Alpine meadow consists mainly of *Kobresia* species (e.g., *K. littledalei*, *K. royleana*, *Carex moorcroftii*), together with limited abundances of plants from Poaceae (e.g., *Stipa purpurea*), *Artemisia* and Chenopodiaceae (e.g., *Chenopodium hybridum*). Montane coniferous

forest (mainly of *Pinus*, *Abies* and *Picea*, mixed with shrubs of *Rhododendron*) and subalpine deciduous broad-leaved shrubs (e.g., *Salix*, *Potentilla*, *Rhododendron*, *Lonicera*, *Caragana* and *Berberis*) are distributed mainly in the southeastern and eastern margins of the plateau. Alpine/temperate deserts are dominated by Chenopodiaceae species (e.g., *Chenopodium hybridum*) accompanied by *Artemisia*, Poaceae, *Ephedra* and *Nitraria*, which develop mainly in the northwestern margin of the plateau and the Qaidam Basin (Fig. 1; Wang et al., 2006; Wu, 1995).

**Table 1**

Information about fossil pollen records on the Qinghai-Tibetan Plateau (see locations in Fig. 1).

No	Site Names	Lat. (°N)	Long. (°E)	Elev. (m)	Archive type	type	No.* date	Time (ka)	Res.# (yrs)	References
R01	Lake Dahaizi	27.5	102.1	3660	Lake	Digit	3	0–12.4	2500	Li and Liu, 1988
R02	Lake Shayema	28.58	102.22	2400	Lake	Digit	5	11.9	130	Jarvis, 1993
R03	Lake Wuxu	29.15	101.41	3705	Lake	Raw	18	11.9	40	Zhang et al., 2016
R04	Muge Co	30.10	101.80	3780	Lake	Raw	8	0–12	64	Ni et al., 2019
R05	Lake Yidun	30.30	99.55	4470	Lake	Digit	3	13.8	400	Shen et al., 2006
R06	Ren Co	30.73	96.68	4450	Lake	Digit	7	17.0	400	Tang et al., 1999
R07	Lake Naleng	31.11	99.76	4200	Lake	Raw	16	16.4	80	Kramer et al., 2010a, 2010b
R08	Butuo Co	31.60	95.60	4682	Lake	Raw	3	0–11.1	155	Zhang et al., 2015
R09	Hongyuan Baihe	32.80	102.53	3500	Peat	Raw	5	10.0	200	Wang, 1987
R10	Hongyuan	32.80	102.53	3400	Peat	Digit	32	11.5	200	Zhou et al., 2010
R11	No. 2 pit	32.85	103.60	3492	Peat	Digit	9	12.7	200	Yan et al., 1999
R12	Wasong	32.99	103.05	3490	Peat	Digit	9	14.9	400	Yan et al., 1999
R13	Zoige ZB10	33.10	102.70	3470	Peat	Digit	20	10.5	50	Sun et al., 2017
R14	Ximen Co	33.38	101.47	4020	Lake	Raw	17	19.8	200	Herzschuh et al., 2014
R15	Lerzha River	33.40	101.00	4170	Peat	Raw	3	10.6	480	Schlüter and Lehmkühl, 2009
R16	Zoige ZB08	33.45	102.63	3467	Peat	Raw	9	10.3	70	Zhao et al., 2011
R17	Zoige DC	33.90	102.55	3396	Peat	Raw	1	21.1	300	Liu et al., 1995
R18	Zoige RM	33.95	102.35	3400	Peat	Raw	5	8.8	180	Shen et al., 1996
R19	Lake Koucha	34.01	97.24	4540	Lake	Raw	5	15.3	230	Herzschuh et al., 2009a
R20	Ayongwama Co	34.83	98.20	4220	Lake	Digit	2	13.4	550	Cheng et al., 2004
R21	Mabu Co	28.33	89.43	4408	Lake	Digit	16	20	32	Han et al., 2021
R22	Pumoyum Co	28.52	90.40	5010	Lake	Digit	60	3–15.1	160	Nishimura et al., 2014
R23	Peiku Co	28.83	85.33	4590	Lake	Raw	3	5–14.7	100	Huang, 2000
R24	Chen Co	28.90	90.60	4420	Lake	Digit	6	2.6–10	120	Lu et al., 2011
R25	Nangla Lu	29.24	87.22	4480	Wetland	Digit	15	20	500	Miehe et al., 2021
R26	Angrenjin Co	29.80	87.20	4306	Lake	Digit	8	3.6	100	Li et al., 2021b
R27	Qongjiemong	29.81	92.37	4980	Lake	Digit	22	14.0	200	Shen, 2003
R28	Lake Hidden	29.81	92.54	4980	Lake	Digit	3	13.5	500	Tang et al., 1999
R29	Ngion Co	30.47	91.50	4515	Lake	Digit	12	5.9	100	Shen et al., 2008
R30	Wumaqu	30.53	91.38	4370	Peat	Raw	3	12.0	600	Wang et al., 1988
R31	Cuo Na	30.55	91.16	4515	Wetland	Digit	7	8.5	140	Cheung et al., 2014
R32	Dangxiong-8	30.70	91.20	4370	Peat	Digit	3	0–10	475	Wang et al., 1981
R33	Dangxiong-9	30.70	91.20	4270	Peat	Digit	3	0–10	500	Wang et al., 1981
R34	Nam Co	30.75	91.00	4718	Lake	Digit	3	7.6	300	Herrmann et al., 2010
R35	Nam Co	30.75	91.00	4718	Lake	Digit	12	8.3	200	Li et al., 2011
R36	Tangra Yumco	31.00	86.50	4545	Lake	Digit	28	3–17.5	115	Ma et al., 2019a, 2019b
R37	Taro Co	31.15	84.00	4566	Lake	Raw	12	10.2	150	Ma et al., 2014
R38	Ahung Co	31.62	92.07	4450	Lake	Digit	56	4.0–9.9	50	Shen, 2003
R39	Xuguo Co	31.95	90.33	4595	Lake	Digit	4	8.7	170	Shen, 2003
R40	Zigetang Co	32.00	90.90	4560	Lake	Raw	5	10.7	150	Herzschuh et al., 2006
R41	Gounong Co	34.63	92.15	4670	Lake	Raw	3	23.1	180	Shan et al., 1996
R42	Donggi Cona	35.50	98.50	4090	Lake	Raw	13	18.3	240	Wang et al., 2014
R43	Lake Kuhai	35.52	99.31	4150	Lake	Raw	13	17.5	300	Wischniewski et al., 2011
R44	Xiqing Mount.	35.65	101.10	3780	Profile	Raw	11	1.3–8.2	67	Miao et al., 2015
R45	Kunlun-Pass	35.70	95.30	3980	Profile	Digit	2	18	540	Liu et al., 1997
R46	Lake Kusai	35.75	93.00	4475	Lake	Raw	7	3.6	10	Wang et al., 2012
R47	Genggahai	36.10	100.10	2860	Lake	Raw	20	6.3	75	Huang et al., 2017
R48	Lake Dalianhai	36.20	100.40	2850	Lake	Raw	10	16	80	Cheng et al., 2013
R49	Lake Qinghai	36.67	100.52	3200	Lake	Raw	10	18.3	70	Liu et al., 2002
R50	Lake Qinghai	36.67	100.52	3200	Lake	Raw	4	11.8	350	Du et al., 1989
R51	Lake Hurleg	37.28	96.90	2817	Lake	Raw	7	3–12.5	150	Zhao et al., 2007a
R52	Lake Hurleg	37.28	96.90	2817	Lake	Digit	7	0.3–14.1	500	Yu et al., 2021
R53	Lake Luanhaizi	37.59	101.35	3200	Lake	Raw	4	26.1	500	Herzschuh et al., 2005
R54	Dunde ice core	38.10	96.40	5325	Ice core	Raw	n.d.	11.0	200	Liu et al., 1998
R55	Tso Kar	33.31	78.03	4527	Lake	Raw	32	15.1	250	Demske et al., 2009
R56	Bangong Co	33.44	79.12	4300	Lake	Raw	17	10.8	270	van Campo et al., 1996
R57	Lake Yanghu	35.43	84.65	4778	Lake	Raw	2	12.8	700	Zhao et al., 2007b
R58	Sumxi Co	35.50	81.00	5058	Lake	Digit	6	12.7	80	van Campo and Gasse, 1993

No.\*: number of dating controls; Res.#: temporal resolution of fossil pollen data.

### 3. Data and methods

#### 3.1. Fossil pollen dataset

Fossil pollen records were collected from the Qinghai-Tibetan Plateau (QTP) and surrounding areas, based on the following criteria: (1) the record should continuously cover a period of at least 4000 years during the past 15 kyrs, (2) the temporal resolution of the pollen record should be higher than 500 years, and (3) the chronology should be established based on at least three dating results. In total, 58 fossil pollen records were selected, including records mentioned in Cao et al. (2013) and Li et al. (2021a), as well as the latest publications (see locations of the records in Fig. 1 and detailed information in Table 1). Generally, the fossil pollen records are distributed in all vegetation zones on the QTP, although relatively more sites were retrieved from the eastern and southern parts. To increase the spatial resolution, a few records with slightly shorter temporal ranges, lower sample resolutions or fewer dating results were included in the dataset, for instance, records from Lake Angrenjinco (Li et al., 2021b), Lake Kusai (Wang et al., 2012), and Lake Yanghu (Zhao et al., 2007b). Most of the pollen records were published in the past two decades, while 6 records were investigated in the 1980s. Raw pollen data were available from 30 sites, while the remaining 28 records were digitized from published pollen diagrams as restricted by the data availability, which may have suffered from potential uncertainties and loss of rare pollen types. However, the major/key pollen species are always available in published pollen diagrams, providing the necessary dataset to perform the biomization schedule. Generally, the principal variations in individual records were captured and represented, contributing significantly to the fossil pollen dataset and subsequent biome reconstruction. Most records covered the whole Holocene period, while limited number of records were available for the late glacial period. In addition, all the radiocarbon dates reported in the original publications were calibrated and interpolated based on the recently developed Bacon age-depth model (Blaauw and Christen, 2011), to avoid potential chronological biases, except for the ice core record from the Dunde ice cap (Liu et al., 1998) and recent lacustrine records with Bacon based radiocarbon chronologies (e.g., Muge Co, Ni et al., 2019; Mabu Co, Han et al., 2021).

#### 3.2. Biomization procedure

Biomization is an objective method to derive regional vegetation changes from fossil pollen records, which assigns pollen taxa to plant functional types (PFTs) and subsequently to biomes (Prentice et al., 1996; Prentice and Webb, 1998). Generally, each pollen taxon was assigned to one or more PFTs based on the modern ecological and biogeographical knowledge, while characteristic PFTs were further classified into major biomes according to bioclimatic signatures. Subsequently, the affinity score for each biome was calculated as the sum of the square root percentage of each pollen taxon assigned in the biome, while pollen taxa with proportions below 0.5% were not included. The scheme of pollen-PFT-biome assignments was initially established at the global scale (Harrison et al., 2010; Prentice et al., 1996), which was adjusted progressively for biome reconstructions in China (Ni et al., 2010, 2014; Tian et al., 2018). Recently, an updated scheme based on pollen/vegetation data in China was set up, and more alpine biome types (particularly alpine meadow, ALME) were included and classified (Supplementary Table S1, Table S2; Sun et al., 2020), which is supposed to be more suitable for vegetation reconstruction in the QTP compared with previous global models. Considering the wide distribution of alpine biomes on the QTP, such an updated scheme was subsequently selected for the biomization procedure. Accordingly, 158 pollen taxa recovered from the fossil pollen records were assigned to 30 PFTs and 18 biomes (see details in Supplementary Table S1 and Table S2). Biomization reconstruction was accomplished using the PPPBase software (Guiot and Goeury, 1996).

### 4. Results

#### 4.1. Biome reconstructions based on the fossil pollen records

In total, 11 biome types were reconstructed on the QTP during the past 15 kyrs based on 58 fossil pollen records (Figs. 2, 3). Generally, diverse forest biomes were determined, consisting of subtropical mixed forest (WAMF), subtropical broadleaf evergreen forest (STFO), warm temperate mixed forest (TEDE), cool temperate mixed forest (COMX), cold temperate summer green conifer forest (CLDC), and cold temperate evergreen conifer forest (CLEC). The forest biomes show dominant contributions in 12 records along the eastern margin of the plateau (Fig. 3). The alpine grassland biomes, i.e., alpine meadow (ALME) and alpine steppe (ALST), were in the eastern and southern parts of the plateau, expressing significant contributions to 6 and 11 records, respectively. Additionally, two types of temperate steppe biomes were assigned with wide distributions (high-frequent appearances in 19 records) on the central and northeastern QTP, including the cool-temperate desert steppe (TEDS) and cool-temperate steppe (STEP). The desert biome (DESE) appeared with high proportions in 10 records, which were mainly from the northwestern QTP and the Qaidam Basin. Generally, the overall spatial distribution of biomes represented the large-scale vegetation gradient on the plateau (see modern vegetation zones in Fig. 1). At the same time, biome reconstruction based on modern pollen data from 1452 sites (after Cao et al., 2014) represents a pattern generally consistent with the distribution of modern vegetation zones on the QTP (see Supplementary Fig. S1). In addition, over 60% of reconstructed biome sequences presented only minor changes during the past 15 kyrs, revealing rather a stable history of regional vegetation changes.

#### 4.2. Reconstructed biome variations on the QTP

During the late glacial period (15–12 ka), relatively few records were recovered, particularly for the period before 14 ka (Figs. 3m-p; Supplementary Fig. S2). The forest biomes were restricted in the southeastern corner of the QTP, showing minor expansions along the eastern edge of the plateau. Similarly, the alpine grassland biomes (ALST and ALME) appeared mainly in the southeastern part of the QTP, with relatively lower frequencies. Comparably, biomes of STEP and DESE showed rather wide distributions on the plateau, especially the appearances of DESE on central and southern parts of the QTP.

Entering the early Holocene (11–8 ka), the number of available pollen records increased greatly, providing more details about spatial patterns in reconstructed biomes (Figs. 3i-l; Supplementary Fig. S2). Generally, the forest biomes were concentrated in the eastern and southern marginal areas of the plateau, where CLEC was distributed in the eastern plateau, while COMX appeared in the southeastern corner. Additionally, a gradual expansion of the forest biomes could be identified along the eastern margin of the plateau. The number of recorded ALME increased during this period, which were mainly from the southern plateau and the Zoige Basin. ALST appeared frequently at high altitudes in the southern plateau together with minor variations. However, temperate steppe communities (STEP and TEDS) were widely determined, which were expressed as the transitional zone between the alpine grasslands and the deserts. In addition, a large number of records with DESE were recovered from the northwestern plateau and the Qaidam Basin.

During the mid-Holocene (8–4 ka), the forest biomes remained at relatively high levels, revealing slight expansions of conifer forest (CLEC) to the northeastern plateau between 7 and 6 ka (Figs. 3e-h; Supplementary Fig. S2). A westward expansion of forests to higher altitudes was recorded as well. The number of assigned ALME declined gradually, which appeared mainly in the southern part of the QTP. The steppe biomes (both ALST and STEP) showed remarkable increases, especially the notable expansion of ALST to the southern QTP. The

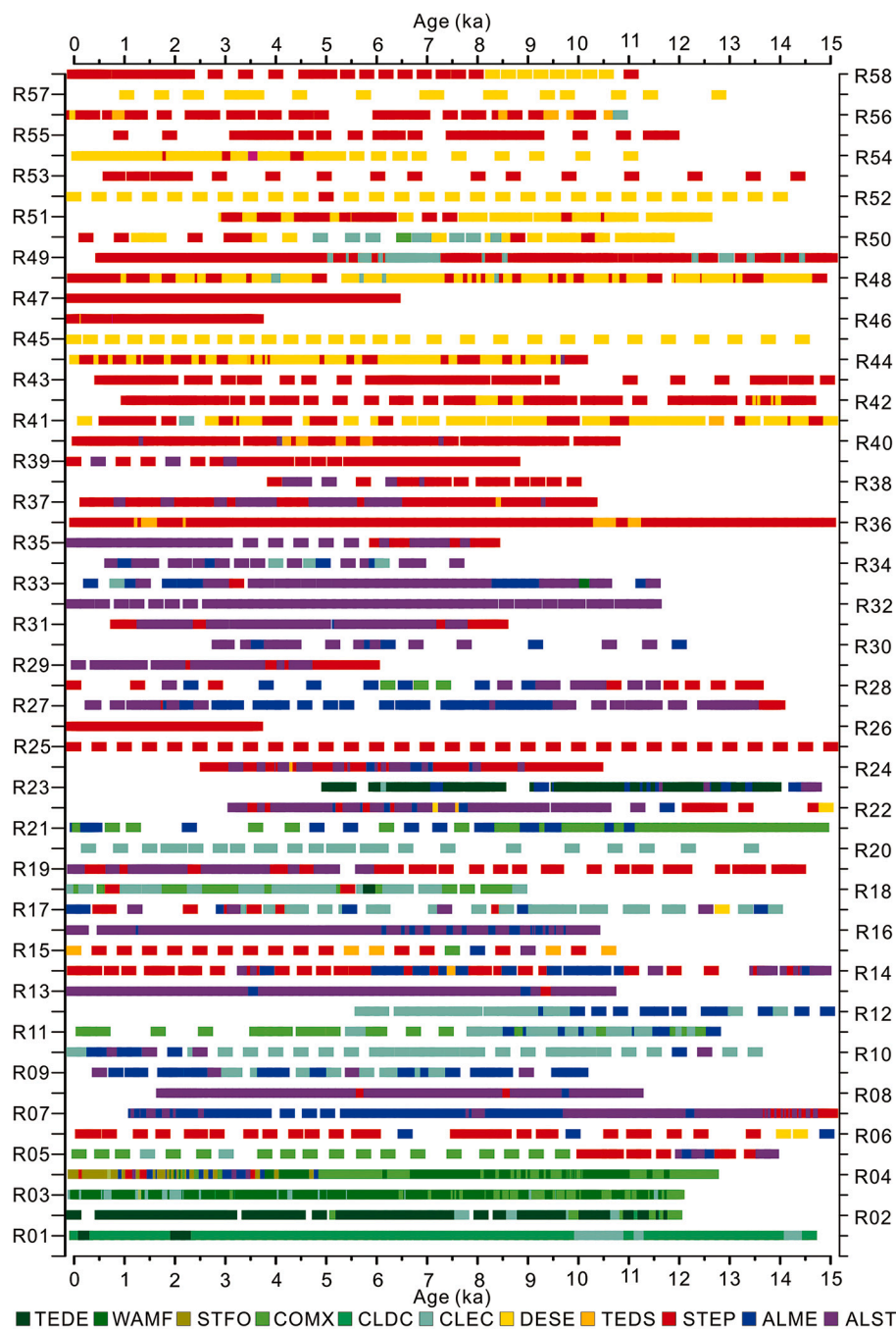


**Fig. 2.** Reconstructed biome sequences for the selected 58 fossil pollen records during the past 15 kyrs. (Abbreviations for the biomes: TEDE, warm-temperate mixed forest; WAMF, north subtropical mixed forest; STFO, south subtropical broadleaf evergreen; COMX, cool-temperate mixed forest; CLDC, cold-temperate summer green conifer forest; CLEC, cold-temperate evergreen conifer forest; DESE, desert; TEDS, cool-temperate desert steppe; STEP, cool-temperate steppe; ALME, alpine meadow; ALST, alpine steppe). (For interpretation of the references to colour in this figure legend, the reader is referred to the web version of this article.)

number of DESE-dominant records declined slightly, and was replaced greatly by STEP in the northern plateau.

For the late Holocene period (after 4 ka), the forest biomes obviously retreated to the southeastern QTP, which were replaced largely by ALME and ALST biomes on the eastern margin of the plateau (Figs. 3a-d; Supplementary Fig. S2). Accordingly, records with ALME were restricted in the eastern plateau while the southern QTP was occupied by ALST and STEP groups. The region dominated by the STEP extended broadly to the eastern and southern parts of the plateau, while DESE appeared mainly in the Qaidam Basin and surrounding areas.

#### 4.3. Holocene biome migrations on the QTP

To detect potential vegetation migrations on the plateau, the distribution of reconstructed biomes along latitude, longitude and altitude

gradients was evaluated and illustrated (Fig. 4; further details are provided in Supplementary Fig. S3 and Fig. S4). Owing to relatively lower number of records during the late glacial period, the examination of vegetation migrations focused mainly on the Holocene period.

The forest biomes expressed gradual expansions during the early to mid-Holocene (until 7 ka; Fig. 4a). Generally, the forests expanded towards higher latitudes (northwards) and lower longitudes (westward), together with fluctuations in altitudes. The distribution of forests between 11 and 9 ka was restricted to relatively lower latitudes with a median value of 30.5°N. The forest progressively moved northwards from 8.5 to 5 ka, reaching a median latitude of approximately 33°N, which retreated gradually after 5 ka towards modern conditions. At the same time, the longitudinal extent of forest spread further west between 11 and 7 ka, and retreated gradually afterwards to the present distributions. Along the altitude, the forest showed frequent vertical

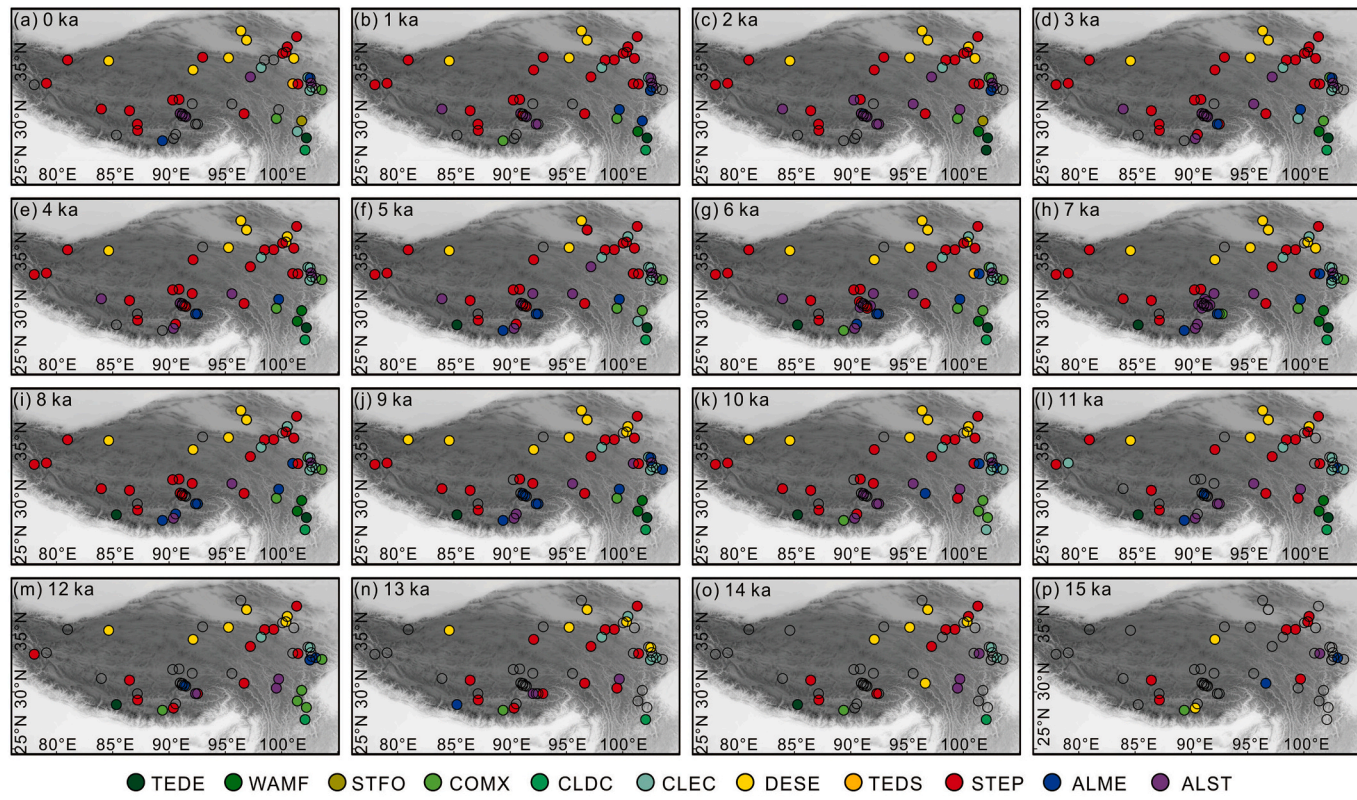


**Fig. 3.** Distribution of reconstructed biomes on the Qinghai-Tibetan Plateau since 15 ka (see maps at 500-year intervals in Supplementary Fig. S2, pollen sites without data were marked as open circles; Abbreviations for the biomes: TEDE, warm-temperate mixed forest; WAMF, north subtropical mixed forest; STFO, south subtropical broadleaf evergreen; COMX, cool-temperate mixed forest; CLDC, cold-temperate summer green conifer forest; CLEC, cold-temperate evergreen conifer forest; DESE, desert; TEDS, cool-temperate desert steppe; STEP, cool-temperate steppe; ALME, alpine meadow; ALST, alpine steppe). (For interpretation of the references to colour in this figure legend, the reader is referred to the web version of this article.)

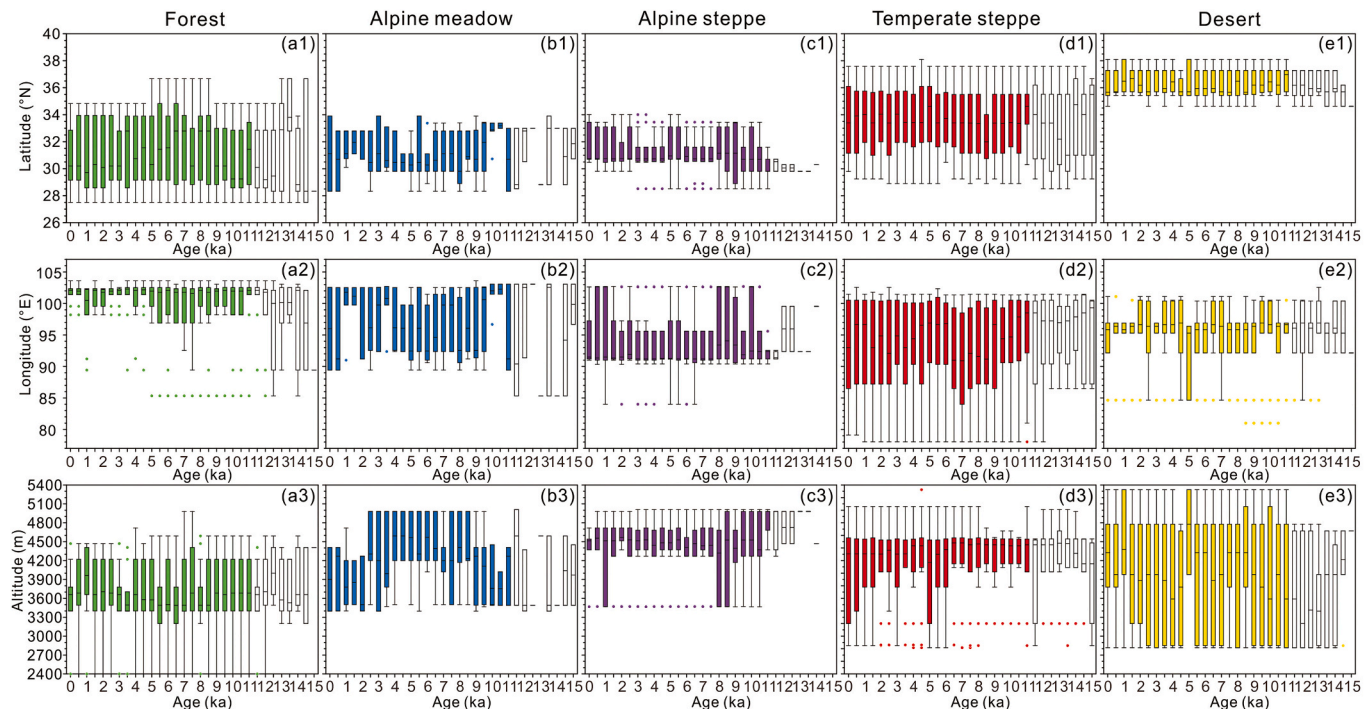


**Fig. 4.** Variations in vegetation groups of forest (a), alpine meadow (b), alpine steppe (c), temperate steppe (d) and desert (e) along gradients of latitude, longitude, and altitude (The columns in the figure represent different vegetation groups, while rows indicate temporal patterns along latitude, longitude and altitude gradients, respectively; the data limits of boxplots were set to 25 and 75 percentiles, while the period between 15 and 12 ka were marked as open boxes owing to higher uncertainties caused by limited number of pollen records).

variations together with a slight expansion to low altitudes (mainly in the Zoige Basin) during the mid-Holocene.

Remarkable migration patterns were determined for ALME, in both the horizontal and vertical directions (Fig. 4b). There was an obvious trend of southward migration during the early Holocene, along with a gradual westward expansion, which generally represented the variations from the eastern to southern plateau. Vertically, the altitude range of ALME increased significantly, reaching up to nearly 5000 m a.s.l. at approximately 8 ka. Such a situation was maintained during the mid-Holocene period, while the migration of ALME back towards the eastern/northern QTP as well as relatively lower altitudes occurred at approximately 4 ka.

The overall migration pattern of ALST was consistent with ALME, despite slight differences in the changing time points (Fig. 4c). Generally, ALST exhibited horizontal migrations towards low latitudes/longitudes, along with a vertical trend to high altitudes after entering the Holocene, which returned during the late Holocene period after 3 ka. However, only minor migration trends were determined for the widely distributed STEP, showing horizontal variation during the early Holocene towards lower latitude/longitude areas (Fig. 4d). In terms of altitude, there was a slight expansion of the STEP to lower altitudes during the late Holocene (after 4 ka). In addition, no clear temporal migration pattern was induced for DESE, possibly owing to the limited number of records (Fig. 4e).

## 5. Discussions

### 5.1. Biome distribution and migration on the QTP

Relatively lower numbers of pollen records were available for the late glacial period (before 11.5 ka), which was dominated by biome types of STEP and DESE (Figs. 2, 3). Forest components were restricted to the southeastern/eastern margins of the QTP during this period, among which, CLDC and CLEC were mainly distributed in the east of the plateau, while COMX, TEDE, WAMF, and STFO appeared in the southeastern part (Fig. 3, and Supplementary Fig. S2). The overall vegetation structure on the plateau is broadly consistent with previous biome reconstructions (Li et al., 2019a; Ni et al., 2014; Tian et al., 2018), that biome types of steppe, desert and forb tundra were yielded on the QTP during the late glacial period. With the updated PFT and biome assignments (Sun et al., 2020), the alpine meadow (ALME) was determined, e.g., the Wasong section (R27) on the eastern part of QTP (Yan et al., 1999), which has not yet been identified in previous results based on global biome schemes. Accordingly, a relatively open landscape could be deduced for such a period before the Holocene, illustrating comparable results with the previous reconstructions for the Last Glacial Maximum (LGM) period (CQPD, 2000; Li et al., 2019b; Ni et al., 2010; Yu et al., 2000).

During the early Holocene between 11.5 and 8 ka, more fossil pollen records were available, particularly for the areas dominated by temperate steppe (STEP) and alpine steppe (ALST) on the southern and southeastern QTP (Figs. 2, 3). Generally, STEP and ALST are distributed widely on the plateau, which is broadly consistent with previous reconstructions on the QTP, despite relatively lower resolutions (Li et al., 2019a; Ni et al., 2014; Tian et al., 2018). Notable expansion of forest could be deduced based on the spatial distribution and temporal variations of the forest biomes (e.g., CLEC, COMX; Figs. 3–5), which is briefly consistent with the increase in forest extent based on synthesized arboreal pollen abundance on the QTP (Chen et al., 2020). In addition, a northwards shift (migration) of forest biomes during 9–5 ka was determined on the eastern QTP (Cheng et al., 2018). Additionally, the Regional Estimates of Vegetation Abundance from Large Sites (REVEALS) model induced vegetation reconstruction presented an identical pattern, showing increased forest components on the southeastern part of the QTP (Li et al., 2020). Such westward and northwards expansions of the forest biomes were also inferred from simulation results using the

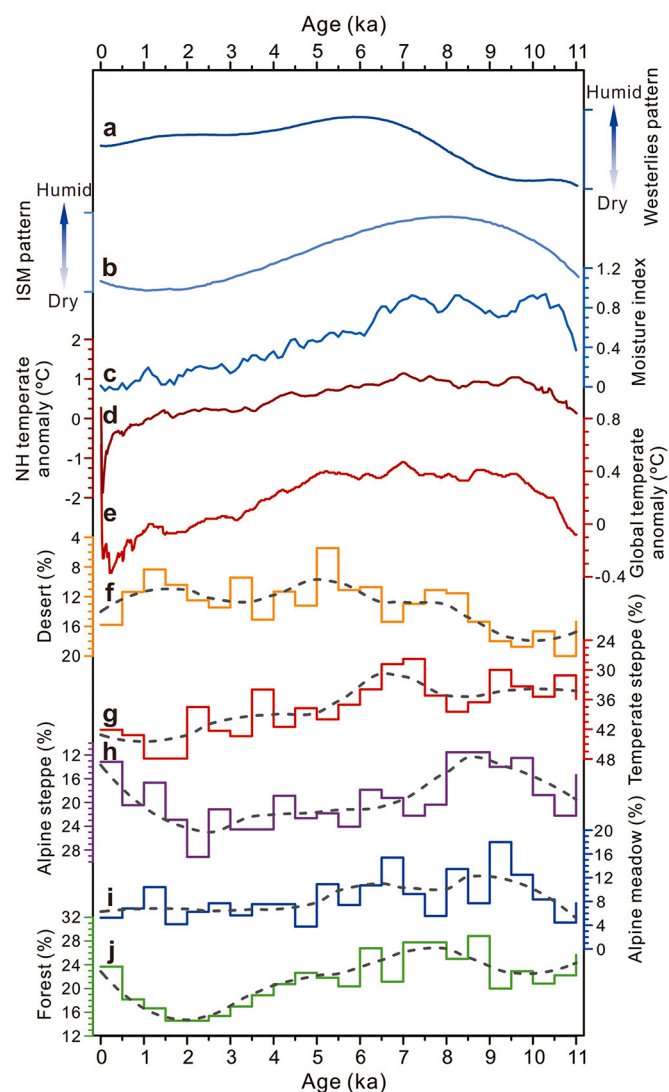


**Fig. 5.** Comparison between the relative proportions of vegetation groups (f–j) with climate records during the Holocene. (a) simplified Westerlies evolution pattern (Chen et al., 2019), (b) simplified Indian Summer Monsoon (ISM) evolution pattern (Chen et al., 2019), (c) averaged moisture index from monsoonal central Asia (Wang et al., 2010), (d) Northern Hemisphere (NH, 30 to 90°N) temperature anomaly (Marcott et al., 2013), (e) global temperature anomaly (Marcott et al., 2013). Dashed lines represent the locally weighted regression (LOESS) smoothing curves.

BIOME4 model, which showed that the tree line moved further north during the early Holocene (Song et al., 2005). Along with the expansions of forest biomes, ALME and ALST communities exhibited obvious westward and southward migrations towards higher altitude regions of the plateau (Figs. 3, 4), which had not yet been detected in previous biomization reconstructions (Li et al., 2019a; Ni et al., 2014; Tian et al., 2018). An increase in alpine meadow components on the southern QTP was also noticed in the synthesized vegetation history of the highland area (i.e., the QTP; Zhao et al., 2009).

In the mid-Holocene (8–4 ka), the proportion of forest biomes declined progressively (Fig. 5j), along with a gradual retreat towards the southeastern plateau (Fig. 4a), revealing a pattern consistent with synthesized arboreal pollen content on the QTP (Chen et al., 2020). Generally, such retreat in forest components was broadly in agreement with large scale biome reconstructions for the mid-Holocene scenario (Li et al., 2019b; Ni et al., 2010; Yu et al., 2000) as well as sequential results (Li et al., 2019a; Ni et al., 2014; Tian et al., 2018), despite relatively

lower temporal/spatial resolutions in previous reconstructions. In addition, cold-temperate evergreen conifer forest (CLEC) was determined from Lake Qinghai on the northeastern margin of the plateau, as revealed by high arboreal pollen proportions in the fossil pollen assemblages (Du et al., 1989; Liu et al., 2002), which declined gradually after ca. 5 ka (Fig. 2; Herzschuh et al., 2009b). Such forest decline was further supported by simulated 6000-year land cover changes in the comprehensive earth system model, in which forest retreated gradually on the northeastern QTP during the late Holocene (Dallmeyer et al., 2011). High proportions of Cyperaceae were recovered in records from the central and southern QTP, indicating the development of alpine meadow (ALME) communities (Li et al., 2016). The occurrence of Cyperaceae in the southern plateau was also reconstructed by the REVEALS model, accounting for over 80% of the regional landscape (Li et al., 2020).

For the late Holocene period after 4 ka, the most pronounced pattern was the expansion of steppe communities (both STEP and ALST), along with further retreats in the biomes of forest and alpine meadow (Fig. 5). Rapid degradation of peatland together with retreat of coniferous forest were noticed in the Zoige Basin (Sun et al., 2017), resulting in subsequent regional biodiversity losses (Liang et al., 2019). The increases in steppe components have been widely noticed from the northeastern and central parts of the QTP (Herzschuh et al., 2009a; Zhao et al., 2009), indicated by high contributions of *Artemisia* pollen. The simulated late Holocene vegetation compositions also captured the dominant contribution of grassland (steppe) on the QTP (Dallmeyer et al., 2011). Additionally, increased steppe components were reconstructed from the northwestern and northeastern QTP based on the REVEALS model (Li et al., 2020), which may account for the expansion of the STEP to lower altitudes (Fig. 4d). The forests experienced a gradual migration back to the eastern margin of the plateau, with elevations below 4000 m (Cheng et al., 2018). ALST and ALME showed movements towards the eastern and northern plateau, following the invasion from STEP communities (Fig. 4), which is generally consistent with the previously reported expansions of temperate grassland and temperate xerophytic shrubland (Ni et al., 2014; Tian et al., 2018).

## 5.2. Factors influencing biome changes on the QTP

Generally, climate changes, including variations in temperature and precipitation (or moisture), have been widely recognized as dominant parameters driving vegetation changes at broad spatial/temporal scales (Cao et al., 2019; Friend et al., 2013; Herzschuh et al., 2009a; Zhao et al., 2009; Zhao and Yu, 2012). The Northern Hemisphere (NH) temperature experienced a progressive increase since the late Glacial, reaching a maximum during the early Holocene (approximately 9–7 ka) and declining gradually afterwards (Marcott et al., 2013; Shakun et al., 2012). Such temperature increases at the transition from the late glacial period to the Holocene played significant roles in the development of vegetation (Li et al., 2019b; Tian et al., 2018). The biomization reconstruction reveals that the forest biomes on the QTP expanded gradually in the early Holocene and reached a maximum between approximately 9–6 ka (Figs. 3, 5), expressing basically consistent pattern with the NH temperature (Fig. 5d; Marcott et al., 2013), despite different Holocene temperature trends (e.g., Liu et al., 2014; Marsicek et al., 2018). Such correlation may suggest that the variations in forest biomes have been potentially influenced by changes in temperature, which has been reported from the investigations of fossil pollen records in the Zoige Basin (Zhao et al., 2011, 2021b). Temperature has been generally considered a constraint on vegetation development, which supplies necessary energy for plant growth (Liu et al., 2010; Walther and Linderholm, 2006). However, owing to the high elevation on the QTP, temperature changes play relatively minor roles in the vastly distributed arid and semi-arid regions, where the development of ecosystems receives more influence from variations in moisture/precipitation (Piao et al., 2006; Sankaran et al., 2005). In addition, the drought stress caused by warming may

even have a negative impact on plant growth considering the intensified evaporation (Cong et al., 2017; Zou et al., 2005). In turn, such complex process may explain the relatively weak correlations between temperature and the non-forest biomes (Fig. 5).

Alternatively, variations in alpine ecosystems are suggested to respond sensitively to changes in precipitation (moisture), considering the overall arid and semi-arid conditions on the QTP (Herzschuh et al., 2009a; Lu et al., 2011; Tang et al., 2021). Generally, the QTP is under the joint influences of the Asian Summer Monsoon systems, including the Indian Summer Monsoon (ISM) and the East Asian Summer Monsoon (EASM), as well as the mid-latitude Westerlies, which led to rather divergent moisture patterns on the plateau (Chen et al., 2020). Intensified ISM and associated increases in monsoonal rainfall were widely reported during the early Holocene (Dykoski et al., 2005; Wang et al., 2005), which declined gradually since the mid-Holocene (Fig. 5b, c; Chen et al., 2019; Wang et al., 2010). Accordingly, the temporal variations in reconstructed forest biomes and alpine meadow exhibited consistent patterns with the ISM intensity (Fig. 5i, j). The steppe biomes (STEP and ALST) represent generally opposite trends with the ISM intensity, showing relatively low proportions during the early Holocene (Fig. 5g, h). The expansions of forest and alpine meadow following increased monsoonal rainfall have possibly led to such retreat of steppe biomes. Therefore, monsoonal precipitation brought by the ISM has significantly controlled the development of alpine ecosystems, as noted in previous investigations (Herzschuh et al., 2009a; Li et al., 2016). However, the maximal EASM occurred during the mid-Holocene according to quantitative precipitation reconstruction (Chen et al., 2015) and synthesized regional moisture patterns (Chen et al., 2019; Wang et al., 2017). The development of forest on the northeastern QTP during the mid-Holocene was deduced from Lake Qinghai (Du et al., 1989; Liu et al., 2002), which indicates the potential response of vegetation to the variation in the EASM (Herzschuh et al., 2009b). In addition, climate conditions in the northwestern and northern parts of the plateau received significant influences from the mid-latitude Westerlies (Chen et al., 2019, 2020), which experienced a progressive increase in moisture during the early to mid-Holocene, followed by a gradual decline after 6 ka according to synthesized palaeoclimate records (Fig. 5a; Chen et al., 2019). Consistent temporal variations could be noticed in the proportion of desert biome, which decreased gradually during the early to mid-Holocene between 11 and 6 ka, owing to increased regional moisture brought by the mid-latitude Westerlies (Fig. 5f). Then, the desert biome expanded slightly during the mid to late Holocene (after approximately 6 ka), responding briefly to the decrease in Westerlies-induced rainfall (Fig. 5a).

Additionally, various non-climate factors were suggested to offer significant influences on past vegetation changes. Modern ecological evidence has revealed that elevated CO<sub>2</sub> concentrations could improve the water use efficiency of plants, especially in arid and semi-arid areas (Gerhard and Ward, 2010; Morgan et al., 2001; Nelson et al., 2004), which has been regarded as a potential driver of Holocene vegetation changes on the QTP (Herzschuh et al., 2011) and even larger spatial scales (Tian et al., 2018). The complex vegetation-climate feedback process may also contribute seriously to regional vegetation changes according to climate simulation results (Chen et al., 2004; Claussen, 1997). Generally, the expansion of dense vegetation may lead to increases in vegetation coverage and corresponding evapotranspiration, increasing the vapour content in the atmosphere and subsequently regional precipitation, which in turn promotes the development of vegetation (Dallmeyer et al., 2010). Regional topography may affect the vegetation distribution through influences on climate conditions or the vertical migration of vegetation zones (Cheng et al., 2018), which should be considered particularly in the southeastern margin of the QTP. In addition, despite the harsh environment on the plateau, the hypothesis of human-induced vegetation change has been proposed during the mid to late Holocene (Hou et al., 2017; Miehe et al., 2014), while debates remain regarding whether human activities have caused serious

vegetation change compared to climate variations (Herzschuh et al., 2009b; Zhao and Yu, 2012). Unfortunately, restricted by the temporal and spatial resolutions of reconstructed biomes, no correlation between the biome changes on the QTP and these non-climate factors was determined, which requires further investigation, as well as systemic long-term model simulations.

In summary, the vegetation variations on the QTP were predominantly controlled by regional moisture conditions, representing divergent spatial patterns. Moisture brought by the ISM promotes the development of alpine ecosystems to a large extent, while the northeastern plateau receives potential influences from the EASM. Alternatively, the deserts respond closely to regional precipitation driven by the Westerlies. The influence of temperature on vegetation was restricted to the forest biomes, while the combined contribution between precipitation and temperature was merely distinguished.

## 6. Conclusions

Based on the biomization method, large-scale vegetation changes on the Qinghai-Tibetan Plateau during the past 15 kyr were quantitatively reconstructed using 58 fossil pollen records, revealing regional biome compositions and potential migration patterns. In general, dominant vegetation biomes on the QTP since the late Glacial have been deduced, consisting of six forest biomes (TEDE, WAMF, STFO, COMX, CLDC and CLEC), alpine meadow (ALME), alpine steppe (ALST), temperate steppe (TEDS, STEP) and desert (DESE). The vegetation distributions represented by reconstructed biomes captured the overall gradient from forests in the southeastern QTP to deserts in the north and northwest. During the Holocene, notable expansions of forest were determined, towards areas of high latitude/low longitude. The alpine meadow and alpine steppe communities expressed consistent migrations to the southern part of the QTP, while minor variations were detected for temperate steppe and desert. Variations in regional precipitation were supposed to be the predominant driving factor for vegetation change on the QTP, while temperature change may have certain influences on the developments of forest biomes. Accordingly, the monsoonal rainfall exhibits significant influences on the biomes ranging from forest, alpine meadow, alpine steppe and temperate steppe. The variations in desert components revealed potential response to moisture changes dominated by the mid-latitude Westerlies. Our results highlight the spatial and temporal variability of alpine ecosystems on the QTP and corresponding responses to climate fluctuations, providing important information for paleoclimate reconstruction and for the prediction of future land cover patterns on the QTP.

## Declaration of Competing Interest

The authors declare that they have no known competing financial interests or personal relationships that could have appeared to influence the work reported in this paper.

## Data availability

Data will be made available on request.

## Acknowledgments

We thank Dr. Enlou Zhang, Dr. Xiaozhong Huang, Dr. Yunfa Miao, Dr. Yun Zhang, Dr. Bo Cheng, Dr. Zhenyu Ni, and other palynologists for providing the original fossil pollen data. The study was financially supported by the National Natural Science Foundation of China (No. 41877282, 41861134030). We are grateful to the editor (Prof. Dr. Howard Falcon-Lang), and the anonymous referees for their constructive suggestions that improved our manuscript.

## Appendix A. Supplementary data

Supplementary data to this article can be found online at <https://doi.org/10.1016/j.palaeo.2022.111190>.

## References

- An, Z.S., Kutzbach, J.E., Prell, W.L., Porter, S.C., 2001. Evolution of Asian monsoon and phased uplift of the Himalaya-Tibetan Plateau since Late Miocene times. *Nature*. 411, 62–66.
- Blaauw, M., Christen, J.A., 2011. Flexible paleoclimate age-depth models using an autoregressive gamma process. *Bayesian Anal.* 6, 457–474.
- Cao, X., Ni, J., Herzschuh, U., Wang, Y., Zhao, Y., 2013. A late quaternary pollen dataset from eastern continental Asia for vegetation and climate reconstructions: set up and evaluation. *Rev. Palaeobot. Palynol.* 194, 21–37.
- Cao, X., Herzschuh, U., Telford, R.J., Ni, J., 2014. A modern pollen-climate dataset from China and Mongolia: assessing its potential for climate reconstruction. *Rev. Palaeobot. Palynol.* 211, 87–96.
- Cao, X., Tian, F., Dallmeyer, A., Herzschuh, U., 2019. Northern Hemisphere biome changes (>30°N) since 40 cal ka BP and their driving factors inferred from model-data comparisons. *Quat. Sci. Rev.* 220, 291–309.
- Chang, D.H.S., 1983. The Tibetan Plateau in relation to the vegetation of China. *Ann. Mo. Bot. Gard.* 70, 564–570.
- Chen, M., Pollard, D., Barron, E.J., 2004. Regional climate change in East Asia simulated by an interactive atmosphere soil vegetation model. *J. Clim.* 17 (3), 557–572.
- Chen, F., Xu, Q., Chen, J., Birks, H.J., Liu, J., Zhang, S., Jin, L., An, C., Telford, R.J., Cao, X., Wang, Z., Zhang, X., Selvaraj, K., Lu, H., Li, Y., Zheng, Z., Wang, H., Zhou, A., Dong, G., Zhang, J., Huang, X., Bloemendal, J., Rao, Z., 2015. East Asian summer monsoon precipitation variability since the last deglaciation. *Sci. Rep.* 5, 11186.
- Chen, F., Chen, J., Huang, W., Chen, S., Huang, X., Jin, L., Jia, J., Zhang, X., An, C., Zhang, J., Zhao, Y., Yu, Z., Zhang, R., Liu, J., Zhou, A., Feng, S., 2019. Westerlies Asia and monsoonal Asia: Spatiotemporal differences in climate change and possible mechanisms on decadal to sub-orbital timescales. *Earth-Sci. Rev.* 192, 337–354.
- Chen, F., Zhang, J., Liu, J., Cao, X., Hou, J., Zhu, L., Xu, X., Liu, X., Wang, M., Wu, D., Huang, L., Zeng, T., Zhang, S., Huang, W., Zhang, X., Yang, K., 2020. Climate change, vegetation history, and landscape responses on the Tibetan Plateau during the Holocene: a comprehensive review. *Quat. Sci. Rev.* 243, 106444.
- Cheng, J., Zhang, X., Tian, M., Tang, D., Yu, W., Yu, J., Qiao, G., Zan, L., 2004. Climate of the Holocene megathermal in the source area of the Yellow River, Northeast Tibet. *Geological Rev.* 3, 330–337 (in Chinese with English abstract).
- Cheng, B., Chen, F., Zhang, J., 2013. Palaeovegetational and palaeoenvironmental changes since the last deglacial in Gonghe Basin, northeast Tibetan Plateau. *J. Geogr. Sci.* 23, 136–146.
- Cheng, Y., Liu, H., Wang, H., Hao, Q., 2018. Differentiated climate-driven Holocene biome migration in western and eastern China as mediated by topography. *Earth-Sci. Rev.* 182, 174–185.
- Cheung, M., Zong, Y., Zheng, Z., Huang, K., Aitchison, J.C., 2014. A stable mid-late Holocene monsoon climate of the central Tibetan Plateau indicated by a pollen record. *Quat. Int.* 333, 40–48.
- Claussen, M., 1997. Modeling biogeophysical feedback in the African and Indian monsoon region. *Clim. Dyn.* 13, 247–257.
- Claussen, M., Brovkin, V., Ganopolski, A., 2001. Biogeophysical versus biogeochemical feedbacks of large-scale land cover change. *Geophys. Res. Lett.* 28, 1011–1014.
- Cong, N., Shen, M., Yang, W., Yang, Z., Zhang, G., Piao, S., 2017. Varying responses of vegetation activity to climate changes on the Tibetan Plateau grassland. *Int. J. Biometeorol.* 61, 1433–1444.
- CQPD (Members of China Quaternary Pollen Data Base), 2000. Pollen-based biome reconstruction at middle Holocene (6 ka BP) and last glacial maximum (18 ka BP) in China. *Acta Bot. Sin.* 42, 1201–1209.
- Dallmeyer, A., Claussen, M., Otto, J., 2010. Contribution of oceanic and vegetation feedbacks to Holocene climate change in monsoonal Asia. *Clim. Past* 6, 195–218.
- Dallmeyer, A., Claussen, M., Herzschuh, U., Fischer, N., 2011. Holocene vegetation and biomass changes on the Tibetan Plateau—a model-pollen data comparison. *Clim. Past* 7, 881–901.
- Demske, D., Tarasov, P.E., Wuehnemann, B., Riedel, F., 2009. Late Glacial and Holocene vegetation, Indian monsoon and westerly circulation in the Trans-Himalaya recorded in the lacustrine pollen sequence from Tso Kar, Ladakh, NW India. *Paleogeogr. Palaeoclimatol. Paleocool.* 279, 172–185.
- Du, N., Kong, Z., Shan, F., 1989. A preliminary investigation on the vegetational and climatic changes since 11000 years in Qinghai Lake—An analysis based on palynology in core QH85. *Acta Bot. Sin.* 31, 803 (in Chinese with English abstract).
- Dykoski, C.A., Edwards, R.L., Cheng, H., Yuan, D., Cai, Y., Zhang, M., Lin, Y., Qing, J., An, Z., Revenaugh, J., 2005. A high-resolution, absolute-dated Holocene and deglacial Asian monsoon record from Dongge Cave, China. *Earth Planet. Sci. Lett.* 233, 71–86.
- ECVC (Editorial Committee for Vegetation of China), Editorial Committee of Vegetation of China, 1980. *Vegetation of China*. Science Press, Beijing (in Chinese).
- Edwards, K.J., Fyfe, R.M., Jackson, S.T., 2017. The first 100 years of pollen analysis. *Nat. Plant* 3, 17001.
- Elenga, H., Peyron, O., Bonnefille, R., Jolly, D., Cheddadi, R., Guiot, J., Andrieu, V., Bottema, S., Buchet, G., de Beaulieu, J.L., Hamilton, A.C., Maley, J., Marchant, R., Perez-Obiol, R., Reille, M., Riollet, G., Scott, L., Straka, H., Taylor, D., Van Campo, E., Vincens, A., Laarif, F., Jonson, H., 2000. Pollen-based biome

- reconstruction for southern Europe and Africa 18 000 yr BP. *J. Biogeogr.* 27, 621–634.
- Friend, A.D., Lucht, W., Rademacher, T.T., Keribin, R., Betts, R., Cadule, P., Ciais, P., Clark, D.B., Dankers, R., Falloon, P.D., Ito, A., Kahana, R., Kleidon, A., Lomas, M.R., Nishina, K., Ostberg, S., Pavlick, R., Peylin, P., Schaphoff, S., Vuichard, N., Warszawski, L., Wiltshire, A., Woodward, I., 2013. Carbon residence time dominates uncertainty in terrestrial vegetation responses to future climate and atmospheric CO<sub>2</sub>. *Proc. Natl. Acad. Sci. U. S. A.* 111, 3280–3285.
- Gerhard, L.M., Ward, J.K., 2010. Plant responses to low CO<sub>2</sub> of the past. *New Phytol.* 188, 674–695.
- Gruet, J., Goeury, C., 1996. PPPbase, a software for statistical analysis of paleoecological and paleoclimatological data. *Dendrochronologica*. 14, 295–300.
- Han, J., Cai, M., Shao, Z., Liu, F., Zhang, Q., Zhang, S., Yu, J., Li, X., Zhang, Z., Zhu, D., 2021. Vegetation and climate change since the late glacial period on the southern Tibetan Plateau. *Paleogeogr. Paleoclimatol. Paleoecol.* 572, 110403.
- Harrison, S.P., Prentice, I.C., Sutera, J.P., Barbón, D., Kohfeld, K.E., Ni, J., 2010. Towards a global scheme of plant functional types for ecosystem modelling, palaeoecology and climate impact research. *J. Veg. Sci.* 21, 300–317.
- Herrmann, M., Lu, X., Berking, J., Schuett, B., Yao, T., Mosbrugger, V., 2010. Reconstructing Holocene vegetation and climate history of Nam Co area (Tibet), using pollen and other palynomorphs. *Quat. Int.* 218 (1–2), 45–57.
- Herzschuh, U., Zhang, C., Mischke, S., Herzschuh, R., Mohammadi, F., Mingram, B., Kürschner, H., Riedel, F., 2005. A late quaternary lake record from the Qilian Mountains (NE China): evolution of the primary production and the water depth reconstructed from macrofossil, pollen, biomarker, and isotope data. *Glob. Planet. Chang.* 46 (1–4), 361–379.
- Herzschuh, U., Winter, K., Wueemann, B., Li, S., 2006. A general cooling trend on the central Tibetan Plateau throughout the Holocene recorded by the Lake Zigaretang pollen spectra. *Quat. Int.* 154–155, 113–121.
- Herzschuh, U., Kramer, A., Mischke, S., Zhang, C., 2009a. Quantitative climate and vegetation trends since the late glacial on the northeastern Tibetan Plateau deduced from Koucha Lake pollen spectra. *Quat. Res.* 71, 162–171.
- Herzschuh, U., Birks, H.J.B., Liu, X., Kubatzki, C., Lohmann, G., 2009b. What caused the mid-Holocene forest decline on the eastern Tibet-Qinghai Plateau? *Glob. Planet. Chang.* 19, 278–286.
- Herzschuh, U., Ni, J., Birks, J.B., Boehner, J., 2011. Driving forces of mid-Holocene vegetation shifts on the upper Tibetan Plateau, with emphasis on changes in atmospheric CO<sub>2</sub> concentrations. *Quat. Sci. Rev.* 30, 1907–1917.
- Herzschuh, U., Borkowski, J., Schwabe, J., Mischke, S., Tian, F., 2014. Moisture-advection feedback supports strong early-to-mid Holocene monsoon climate on the eastern Tibetan Plateau as inferred from a pollen-based reconstruction. *Paleogeogr. Paleoclimatol. Paleoecol.* 402, 44–54.
- Hou, X., 2001. *Vegetation Atlas of China*. Science Press, Beijing (in Chinese).
- Hou, G., Yang, P., Cao, G., Chongyi, E., Wang, Q., 2017. Vegetation evolution and human expansion on the Qinghai-Tibet Plateau since the last Deglaciation. *Quat. Int.* 430, 82–93.
- Huang, F., 2000. Vegetation and climate between 13 ka to 5ka B.P. in Peiku Co, Tibet. *Acta Palaeontol. Sin.* 3, 441–448 (in Chinese with English abstract).
- Huang, X., Liu, S., Dong, G., Qiang, M., Bai, Z., Zhao, Y., Chen, F., 2017. Early human impacts on vegetation on the northeastern Qinghai-Tibetan Plateau during the middle to late Holocene. *Prog. Phys. Geogr.* 41 (3), 286–301.
- Immerzeel, W.W., Lutz, A.F., Andrade, M., Bahl, A., Biemans, H., Bolch, T., Hyde, S., Brumby, S., Davies, B.J., Elmore, A.C., Emmer, A., Feng, M., Fernandez, A., Haritashya, U., Kargel, J.S., Koppes, M., Kraaijenbrink, P.D.A., Kulkarni, A.V., Mayewski, P.A., Nepal, S., Pacheco, P., Painter, T.H., Pellicciotti, F., Rajaram, H., Rupper, S., Sinisalo, A., Shrestha, A.B., Vivioli, D., Wada, Y., Xiao, C., Yao, T., Baillie, J.E.M., 2020. Importance and vulnerability of the world's water towers. *Nature*. 577, 364–369.
- Izumi, K., Lézine, A.-M., 2016. Pollen-based biome reconstructions over the past 18,000 years and atmospheric CO<sub>2</sub> impacts on vegetation in equatorial mountains of Africa. *Quat. Sci. Rev.* 152, 93–103.
- Jarvis, D.I., 1993. Pollen evidence of changing Holocene monsoon climate in Sichuan province, China. *Quat. Res.* 39, 325–337.
- Kaplan, J., Bigelow, N., Prentice, I., Harrison, S., Bartlein, P., Christensen, T., Cramer, W., Matveyeva, N.V., McGuire, A.D., Murray, D.F., Razzhivin, V.Y., Smith, B., Walker, D.A., Anderson, P.M., Andreev, A.A., Brubaker, L.B., Edwards, M.E., Lozhkin, A.V., 2003. Climate change and Arctic ecosystems II: modeling paleodata-model comparisons and future projections. *J. Geophys. Res.* 108, 8171.
- Kramer, A., Herzschuh, U., Mischke, S., Zhang, C., 2010a. Holocene treeline shifts and monsoon variability in the Hengduan Mountains (southeastern Tibetan Plateau) implications from palynological investigations. *Paleogeogr. Paleoclimatol. Paleoecol.* 286, 23–41.
- Kramer, A., Herzschuh, U., Mischke, S., Zhang, C., 2010b. Late glacial vegetation and climate oscillations on the southeastern Tibetan Plateau inferred from the Lake Naleng pollen profile. *Quat. Res.* 73, 324–335.
- Li, X., Liu, J., 1988. Holocene vegetational and environmental changes at Mt. Luoji, Sichuan. *Acta Geograph. Sin.* 1, 44–51 (in Chinese with English abstract).
- Li, Q., Lu, H., Zhu, L., Wu, N., Wang, J., Lu, X., 2011. Pollen-inferred climate changes and vertical shifts of alpine vegetation belts on the northern slope of the Nyainqntanglha Mountains (central Tibetan Plateau) since 8.4 kyr BP. *Holocene*. 21, 939–950.
- Li, Q., Lu, H., Shen, C., Zhao, Y., Ge, Q., 2016. Vegetation successions in response to Holocene climate changes in the central Tibetan Plateau. *J. Arid Environ.* 125, 136–144.
- Li, Q., Wu, H., Yu, Y., Sun, A., Luo, Y., 2019a. Large-scale vegetation history in China and its response to climate change since the Last Glacial Maximum. *Quat. Int.* 500, 108–119.
- Li, Q., Wu, H., Yu, Y., Sun, A., Luo, Y., 2019b. Quantifying regional vegetation changes in China during three contrasting temperature intervals since the last glacial maximum. *J. Asian Earth Sci.* 174, 23–36.
- Li, F., Gaillard, M.J., Cao, X., Herzschuh, U., Sugita, S., Tarasov, P.E., Wagnere, M., Xu, Q., Ni, J., Wang, W., Zhao, Y., An, C., Beusen, A.H.W., Chen, F., Feng, Z., Goldewijk, C.G.M.K., Huang, X., Li, Y., Liu, H., Sun, A., Yao, Y., Zheng, Z., Jia, X., 2020. Towards quantification of Holocene anthropogenic land-cover change in temperate China: a review in the light of pollen-based REVEALS reconstructions of regional plant cover. *Earth-Sci. Rev.* 203, 103119.
- Li, Z., Wang, Y., Herzschuh, U., Cao, X., Ni, J., Zhao, Y., 2021a. Pollen-based mapping of Holocene vegetation on the Qinghai-Tibetan Plateau in response to climate change. *Paleogeogr. Paleoclimatol. Paleoecol.* 573, 110412.
- Li, H., Xu, D., Shen, C., Cui, A., Zu, X., Dong, Y., Wang, C., Jin, Y., Yu, Y., Wu, N., Lu, H., 2021b. Multi-centennial climate cycles and their impact on the Tubo Dynasty in the southern Tibetan Plateau. *Paleogeogr. Paleoclimatol. Paleoecol.* 578, 110584.
- Liang, C., Zhao, Y., Qin, F., Cui, Q.-Y., Li, Q., Li, H., Zhang, Z.-Y., 2019. Complex responses of vegetation diversity to Holocene climate change in the eastern Tibetan Plateau. *Veg. Hist. Archaeobotany* 28, 379–390.
- Liu, G., Shen, Y., Wang, S., 1995. The vegetation and climate of Holocene megathermal in Zoige, Northwestern Sichuan, China. *J. Glaciol. Geocryol.* 3, 247–249 (in Chinese with English abstract).
- Liu, G., Cui, Z., Wu, Y., Xu, Q., 1997. Record of environmental change in Reshui profile at Kunlunshan Pass since 18 ka BP. *Int. J. Geomech.* 4, 41–47 (in Chinese with English abstract).
- Liu, K., Yao, Z., Thompson, L.G., 1998. A pollen record of Holocene climatic changes from the Dunde ice cap, Qinghai-Tibetan Plateau. *Geology*. 26, 135–138.
- Liu, X., Shen, J., Wang, S., Yang, X., Tong, G., Zhang, E., 2002. A 16000-year pollen record of Qinghai Lake and its paleoclimate and paleoenvironment. *Chin. Sci. Bull.* 47, 1931–1936.
- Liu, B.H., Henderson, M., Zhang, Y.D., Xu, M., 2010. Spatiotemporal change in China's climatic growing season: 1955–2000. *Clim. Chang.* 99, 93–118.
- Liu, Z., Zhu, J., Rosenthal, Y., Zhang, X., Otto-Biesner, B.L., Timmermann, A., Smith, R.S., Lohmann, G., Zheng, W.P., Timm, O.E., 2014. The Holocene temperature conundrum. *Proc. Natl. Acad. Sci. U. S. A.* 111, 3501–3505.
- Liu, J., Milne, R.J., Zhu, G.F., Spicer, R.A., Wambulwa, M.C., Wu, Z.Y., Boufford, D.E., Luo, Y.H., Provan, J., Yi, T.S., Cai, J., Wang, H., Gao, L.M., L., D.Z., 2022. Name and scale matter: clarifying the geography of Tibetan Plateau and adjacent mountain regions. *Glob. Planet. Chang.* 215, 103893.
- Lu, H., Wu, N., Liu, K.B., Zhu, L., Yang, X., Yao, T., Wang, L., Li, Q., Liu, X., Shen, C., Li, X., Tong, G., Jiang, H., 2011. Modern pollen distributions in Qinghai-Tibetan Plateau and the development of transfer functions for reconstructing Holocene environmental changes. *Quat. Sci. Rev.* 30, 947–966.
- Ma, Q., Zhu, L., Lu, X., Guo, Y., Ju, J., Wang, J., Wang, Y., Tang, L., 2014. Pollen-inferred Holocene vegetation and climate histories in Taro Co, southwestern Tibetan Plateau. *Chin. Sci. Bull.* 59, 4101–4114.
- Ma, Q., Zhu, L., Lu, X., Wang, J., Ju, J., Kasper, T., Daut, G., Haberzettl, T., 2019a. Late Glacial and Holocene vegetation and climate variations at Lake Tangra Yumco, central Tibetan Plateau. *Glob. Planet. Chang.* 174, 16–25.
- Ma, Q., Zhu, L., Wang, J., Ju, J., Wang, Y., Lu, X., Kasper, T., Haberzettl, T., 2019b. Late Holocene vegetation responses to climate change and human impact on the central Tibetan Plateau. *Sci. Total Environ.* 708, 135370.
- Marcott, S.A., Shakun, J.D., Clark, P.U., Mix, A.C., 2013. A reconstruction of regional and global temperature for the past 11300 years. *Science*. 339, 1198–1201.
- Marquer, L., Gaillard, M.J., Sugita, S., Trondman, A.K., Mazier, F., Nielsen, A.B., Fyfe, R., Odgaard, B.V., Alenius, T., B-Birks, H.J., Bjune, A.E., Christiansen, J., Dodson, J., Edwards, K.J., Giesecke, T., Herzschuh, U., Kangur, M., Lorenz, S., Poska, A., Schult, M., Seppä, H., 2014. Holocene changes in vegetation composition in northern Europe: why quantitative pollen-based vegetation reconstructions matter. *Quat. Sci. Rev.* 90, 199–216.
- Marsicek, J., Shuman, B.N., Bartlein, P.J., Shafer, S.L., Brewer, S., 2018. Reconciling divergent trends and millennial variations in Holocene temperatures. *Nature*. 554, 92–96.
- Miao, Y., Jin, H., Liu, B., Herrmann, M., Sun, Z., Wang, Y., 2015. Holocene climate change on the northeastern Tibetan Plateau inferred from mountain-slope pollen and non-pollen palynomorphs. *Rev. Palaeobot. Palynol.* 221, 22–31.
- Miehe, G., Miehe, S., Bohner, J., Kaiser, K., Hensen, I., Madsen, D.B., Liu, J., Ogenoorth, L., 2014. How old is the human footprint in the world's largest alpine ecosystem? A review of multiproxy records from the Tibetan Plateau from the ecologists' viewpoint. *Quat. Sci. Rev.* 86, 190–209.
- Miehe, G., Hasson, S.U., Glaser, B., Mischke, S., Böhne, J., Knaap, W.O., Leeuwen, J.F.N., Duo, L., Miehe, S., Haberzettl, T., 2021. Föhn, fire and grazing in Southern Tibet? A 20,000-year multi-proxy record in an alpine ecotonal ecosystem. *Quat. Sci. Rev.* 256, 106817.
- Morgan, J.A., LeCain, D.R., Mosier, A.R., Milchunas, D.G., 2001. Elevated CO<sub>2</sub> enhances water relations and productivity and affects gas exchange in C<sub>3</sub> and C<sub>4</sub> grasses of the Colorado shortgrass steppe. *Glob. Chang. Biol.* 7, 451–466.
- Nelson, J.A., Morgan, J.A., LeCain, D.R., Mosier, A.R., Milchunas, D.G., Parton, W.J., 2004. Elevated CO<sub>2</sub> increases soil moisture and enhances plant water relations in a long-term field study in the semi-arid shortgrass steppe of Northern Colorado. *Plant Soil* 259, 169–179.
- Ni, J., Herzschuh, U., 2011. Simulating biome distribution on the Tibetan Plateau using a modified global vegetation model. *Arct. Antarct. Alp. Res.* 43, 429–441.

- Ni, J., Yu, G., Harrison, S.P., Colin Prentice, I., 2010. Palaeovegetation in China during the late Quaternary: Biome reconstructions based on a global scheme of plant functional types. *Paleogeogr. Paleoclimatol. Paleoecol.* 289 (1–4), 44–61.
- Ni, J., Cao, X., Jeltsch, F., Herzschuh, U., 2014. Biome distribution over the last 22,000 yr in China. *Paleogeogr. Paleoclimatol. Paleoecol.* 409, 33–47.
- Ni, Z., Jones, R., Zhang, E., Chang, J., Shulmeister, J., Sun, W., Wang, Y., Ning, D., 2019. Contrasting effects of winter and summer climate on Holocene montane vegetation belts evolution in southeastern Qinghai-Tibetan Plateau, China. *Paleogeogr. Paleoclimatol. Paleoecol.* 533, 109232.
- Nishimura, M., Matsunaka, T., Morita, Y., Watanabe, T., Nakamura, T., Zhu, L., Nara, F. W., Imai, A., Izutsu, Y., Hasuike, K., 2014. Paleoclimatic changes on the southern Tibetan Plateau over the past 19,000 years recorded in Lake Pumoyum Co, and their implications for the southwest monsoon evolution. *Paleogeogr. Paleoclimatol. Paleoecol.* 396, 75–92.
- Piao, S., Mohammadi, A., Fang, J., Cai, Q., Feng, J., 2006. NDVI-based increase in growth of temperate grasslands and its responses to climate changes in China. *Glob. Environ. Chang.* 16, 340–348.
- Piao, S., Zhang, X., Wang, T., Liang, E., Wang, S., Zhu, J., Niu, B., 2019. Responses and feedback of the Tibetan Plateau's alpine ecosystem to climate change. *Chin. Sci. Bull.* 64, 2842–2855.
- Prentice, I.C., Webb, T.I.I.I., 1998. BIOME 6000: reconstructing global mid-Holocene vegetation patterns from palaeoecological records. *J. Biogeogr.* 25, 997–1005.
- Prentice, I.C., Cramer, W., Harrison, S.P., Leemans, R., Monserud, R., Solomon, A., 1992. A global biome model based on plant physiology and dominance, soil properties and climate. *J. Biogeogr.* 19, 117–134.
- Prentice, I.C., Guiot, J., Huntley, B., Jolly, D., Cheddadi, R., 1996. Reconstructing biomes from palaeoecological data: a general method and its application to European pollen data at 0 and 6 ka. *Cli. Dynam.* 12, 185–194.
- Prentice, I.C., Harrison, S.J., Jolly, D., Joel, G., 1998. The climate and biomes of Europe at 6000 yr BP: comparison of model simulations and pollen-based reconstructions. *Quat. Sci. Rev.* 17, 659–668.
- Qiu, J., 2008. China: the third pole. *Nature.* 454, 393–396.
- Sankaran, M., Hanan, N.P., Scholes, R.J., Ratnam, J., Zambatis, N., 2005. Determinants of woody cover in African savannas. *Nature.* 438, 846–849.
- Schlüter, F., Lehmkühl, F., 2009. Holocene climatic change and the nomadic Anthropocene in Eastern Tibet: palynological and geomorphological results from the Nianbaoye Mountains. *Quat. Sci. Rev.* 28, 1449–1471.
- Shakun, J.D., Clark, P.U., Marcott, S.A., Mix, A.C., Liu, Z.Y., Otto-Bliesner, B., Schmittner, A., Bard, E., 2012. Global warming preceded by increasing carbon dioxide concentrations during the last deglaciation. *Nature.* 484, 49–54.
- Shan, F., Kong, Z., Du, N., 1996. Palaeovegetation and environmental changes. In: Li, B. (Ed.), *Physical Environment of Hoh Xil Region, Qinghai*. Science Press, Beijing, pp. 197–206 (in Chinese).
- Shen, C., 2003. Millennial-Scale Variations and Centennial-Scale Events in the Southwest Asian Monsoon: Pollen Evidence from Tibet. PhD Dissertation. Louisiana State University.
- Shen, C., Tang, L., Wang, S., 1996. Vegetation and climate during the last 22 000 years in Zoige region. *Acta Micropalaeontol. Sin.* 4, 401–406 (in Chinese with English abstract).
- Shen, C., Liu, K., Tang, L., Overpeck, J.T., 2006. Quantitative relationships between modern pollen rain and climate in the Tibetan Plateau. *Rev. Palaeobot. Palynol.* 140, 61–77.
- Shen, C., Liu, K., Morrill, C., Overpeck, J.T., Peng, J., Tang, L., 2008. Ecotone shift and major droughts during the mid-late Holocene in the central Tibetan Plateau. *Ecology.* 89, 1079–1088.
- Song, M., Zhou, C., Ouyang, H., 2005. Simulated distribution of vegetation types in response to climate change on the Tibetan Plateau. *J. Veg. Sci.* 16, 341–350.
- Sun, H., 1999. *The National Physical Atlas of China*. China Cartographic Publishing House, Beijing (in Chinese).
- Sun, X., Zhao, Y., Li, Q., 2017. Holocene peatland development and vegetation changes in the Zoige Basin, eastern Tibetan Plateau. *Sci. China Earth Sci.* 60, 1826–1837.
- Sun, A., Luo, Y., Wu, H., Chen, X., Li, Q., Yu, Y., Sun, X., Guo, Z., 2020. An updated biomass scheme and vegetation reconstruction based on a synthesis of modern and mid-Holocene pollen data in China. *Glob. Planet. Chang.* 192, 103178.
- Tang, L., Shen, C., Liu, K., Overpeck, J.T., 1999. New high-resolution pollen records from two lakes in Xizang (Tibet). *J. Integr. Plant Biol.* 41, 896–902 (in Chinese with English abstract).
- Tang, L., Shen, C., Lü, H., Li, C., Ma, Q., 2021. Fifty years of Quaternary palynology in the Tibetan Plateau. *Sci. China Earth Sci.* 64, 1825–1843.
- Tian, L., Zhang, Y., Zhu, J., 2014. Decreased surface albedo driven by denser vegetation on the Tibetan Plateau. *Environ. Res. Lett.* 9, 104001.
- Tian, F., Cao, X., Dallmeyer, A., Lohmann, G., Zhang, X., Ni, J., Andreev, A., Anderson, P. M., Lozhkin, A.V., Bezrukova, E., Rudaya, N., Xu, Q., Herzschuh, U., 2018. Biome changes and their inferred climatic drivers in northern and eastern continental Asia at selected times since 40 cal ka BP. *Veg. Hist. Archaeobotany* 27, 365–379.
- van Campo, E., Gasse, F., 1993. Pollen-and diatom-inferred climatic and hydrological changes in Sumxi Co Basin (Western Tibet) since 13,000 yr BP. *Quat. Res.* 39, 300–313.
- van Campo, E., Cour, P., Hang, S., 1996. Holocene environmental changes in Bangong Co Basin (Western Tibet). Part 2: the pollen record. *Paleogeogr. Paleoclimatol. Paleoecol.* 120, 49–63.
- Verrall, B., Pickering, C.M., 2020. Alpine vegetation in the context of climate change: a global review of past research and future directions. *Sci. Total Environ.* 748, 141344.
- Walther, A., Linderholm, H.W., 2006. A comparison of growing season indices for the Greater Baltic Area. *Int. J. Biometeorol.* 51, 107–118.
- Wang, M., 1987. The spore-pollen groups of peatlands on Ruoergai Plateau and paleobotany and paleoclimate. *Sci. Geogr. Sin.* 2, 147–155 (in Chinese with English abstract).
- Wang, P., Xia, Y., Wang, M., 1981. The study on the spore-pollen groups and the evolution of the natural environment of South Xizang Plateau in the peat of the Holocene. *Sci. Geogr. Sin.* 1, 144–152 (in Chinese with English abstract).
- Wang, P., Xia, Y., Wang, M., 1988. An approach to the spore-pollen assemblages of peat in the Holocene and the evolution of natural environment in southern Xizang. In: Huang, X. (Ed.), *Study of Mire in China*. Science Press, Beijing, pp. 257–265 (in Chinese).
- Wang, Y., Cheng, H., Edwards, R.L., He, Y., Kong, X., An, Z., Wu, J., Kelly, M.J., Dykoski, C.A., Li, X., 2005. The Holocene Asian monsoon: links to solar changes and North Atlantic climate. *Science.* 308, 854–857.
- Wang, W., Wang, Q., Li, S., Wang, G., 2006. Distribution and species diversity of plant communities along transect on the northeastern Tibetan Plateau. *Biodivers. Conserv.* 15, 1811–1828.
- Wang, Y., Liu, X., Herzschuh, U., 2010. Asynchronous evolution of the Indian and East Asian Summer Monsoon indicated by Holocene moisture patterns in monsoonal Central Asia. *Earth-Sci. Rev.* 103, 135–153.
- Wang, Y., Liu, X., Herzschuh, U., Yang, X., Birks, H.J.B., Zhang, E., Tong, G., 2012. Temporally changing drivers for late-Holocene vegetation changes on the northern Tibetan Plateau. *Paleogeogr. Paleoclimatol. Paleoecol.* 353–355, 10–20.
- Wang, Y., Herzschuh, U., Shumilovskikh, L.S., Mischke, S., Birks, H.J.B., Wischniewski, J., Boehmer, J., Schlüter, F., Lehmkühl, F., Diekmann, B., Wuennemann, B., Zhang, C., 2014. Quantitative reconstruction of precipitation changes on the NE Tibetan Plateau since the last Glacial maximum-extending the concept of pollen source area to pollen-based climate reconstructions from large lakes. *Clim. Past* 10, 21–39.
- Wang, Y., Bekeschus, B., Handorf, D., Liu, X., Dallmeyer, A., Herzschuh, U., 2017. Coherent tropical-subtropical Holocene see-saw moisture patterns in the Eastern Hemisphere monsoon systems. *Quat. Sci. Rev.* 169, 231–242.
- Williams, J.W., Iii, T.W., Newby, R.P., 2010. Late Quaternary biomes of Canada and the eastern United States. *J. Biogeogr.* 27, 585–607.
- Wischniewski, J., Mischke, S., Wang, Y., Herzschuh, U., 2011. Reconstructing climate variability on the northeastern Tibetan Plateau since the last late Glacial—a multi-proxy, dual-site approach comparing terrestrial and aquatic signals. *Quat. Sci. Rev.* 30, 82–97.
- Wu, Z., 1995. *The Vegetation of China*. Science Press, Beijing (in Chinese).
- Yan, G., Wang, F., Shi, G., Li, S., 1999. Palynological and stable isotopic study of palaeoenvironmental changes on the northeastern Tibetan Plateau in the last 30,000 years. *Paleogeogr. Paleoclimatol. Paleoecol.* 153, 147–159.
- Yasunari, T., 2007. Role of land-atmosphere interaction on Asian Monsoon climate. *J. Meteorol. Soc. Jpn.* 85B, 55–75.
- Yu, G., Prentice, I.C., Sun, X., 1998a. Pollen-based biome reconstructions for China at 0 and 6000 years. *J. Biogeogr.* 25, 1055–1069.
- Yu, G., Sun, X., Qin, B., Song, C., Li, H., Prentice, I.C., Harrison, S.P., 1998b. Pollen-based reconstruction of vegetation patterns of China in mid-Holocene. *Sci. China Earth Sci.* 41, 130–136.
- Yu, G., Chen, X., Ni, J., Cheddadi, R., Joel, G., Han, H., Harrison, S., Huang, C., Ke, M., Kong, Z., Li, S., Li, W., Liew, P., Liu, G., Liu, J., Liu, Q., Liu, K., Prentice, I.C., Qui, W., Ren, G., Song, C., Sugita, S., Sun, X., Tang, L., Vancamp, E., Xia, Y., Xu, Q., Yan, S., Yang, X., Zhao, J., Zheng, Z., 2000. Palaeovegetation of China: a pollen data-based synthesis for the mid-Holocene and last glacial maximum. *J. Biogeogr.* 27, 635–664.
- Yu, Y., Jin, Y., Xu, D., Wang, Y., Li, H., Wang, G., Cui, A., Wei, Z., 2021. Vegetational and climatic changes in the Hurleg Lake, Qinghai, during the last 14000 years. *Quat. Sci.* 41, 1229–1243.
- Zhang, Y., Kong, Z., Zhang, Q., Yang, Z., 2015. Holocene climate events inferred from modern and fossil pollen records in Butuo Lake, Eastern Qinghai-Tibetan Plateau. *Clim. Chang.* 133, 223–235.
- Zhang, E., Wang, Y., Sun, W., Shen, J., 2016. Holocene Asian monsoon evolution revealed by a pollen record from an alpine lake on the southeastern margin of the Qinghai-Tibetan Plateau, China. *Clim. Past* 12, 415–427.
- Zhao, Y., Yu, Z., 2012. Vegetation response to Holocene climate change in East Asian monsoon-margin region. *Earth-Sci. Rev.* 113, 1–10.
- Zhao, Y., Yu, Z., Chen, F., Ito, E., Zhao, C., 2007a. Holocene vegetation and climate history at Hurleg Lake in the Qaidam Basin, Northwest China. *Rev. Palaeobot. Palynol.* 145, 275–288.
- Zhao, Z., Liu, A., Peng, W., 2007b. Holocene environmental changes of northern Qinghai-Tibetan Plateau based on spore-pollen analysis. *Arid Land Geogr.* 3, 381–391 (in Chinese with English abstract).
- Zhao, Y., Yu, Z., Chen, F., Zhang, J., Yang, B., 2009. Vegetation response to Holocene climate change in monsoon-influenced region of China. *Earth-Sci. Rev.* 97, 242–256.
- Zhao, Y., Yu, Z., Zhao, W., 2011. Holocene vegetation and climate histories in the eastern Tibetan Plateau: controls by insolation-driven temperature or monsoon-derived precipitation changes? *Quat. Sci. Rev.* 30, 1173–1184.
- Zhao, P., Zhou, X., Chen, J., Liu, G., Nan, S., 2019. Global climate effects of summer Tibetan Plateau. *Sci. Bull.* 64, 1–3.
- Zhao, D., Zhu, Y., Wu, S., Zheng, D., 2021a. Projection of vegetation distribution to 1.5°C and 2°C of global warming on the Tibetan Plateau. *Glob. Planet. Chang.* 202, 103525.
- Zhao, Y., Liang, C., Cui, Q., Qin, F., Zheng, Z., Xiao, X., Ma, C., Felde, V.A., Liu, Y., Li, Q., Zhang, Z., Herzschuh, U., Xu, Q., Wei, H., Cai, M., Cao, X., Guo, Z., Birks, H.J.B., 2021b. Temperature reconstructions for the last 1.74-Ma on the eastern Tibetan Plateau based on a novel pollen-based quantitative method. *Glob. Planet. Chang.* 199, 103433.

Zheng, D., 1996. The system of physico-geographical regions of the QinghaiXizang (Tibet) Plateau. *Sci. China Earth Sci.* 39, 410–417.

Zhou, W., Yu, S.-Y., Burr, G.S., Kukla, G.J., Jull, A.J.T., Xian, F., Xiao, J., Colman, S.M., Yu, H., Liu, Z., Kong, X., 2010. Postglacial changes in the Asian summer monsoon

system: a pollen record from the eastern margin of the Tibetan Plateau. *Boreas*. 39, 528–539.

Zou, X., Zhai, P., Zhang, Q., 2005. Variations in droughts over China: 1951–2003. *Geophys. Res. Lett.* 32, 353–368.